

Diversity in responses to oncolytic Lassa-vesicular stomatitis virus in patient-derived glioblastoma cells

Teddy E. Kim,¹ Shelby Puckett,² Kailong Zhang,² Denise M. Herpai,³ David A. Ornelles,⁴ John N. Davis,⁵ Anthony N. van den Pol,^{5,6} Waldemar Debinski,³ and Douglas S. Lyles²

¹Department of Neurosurgery, Wake Forest School of Medicine, Winston-Salem, NC, USA; ²Department of Biochemistry, Wake Forest School of Medicine, Medical Center Blvd., Winston-Salem, NC 27157, USA; ³Department of Cancer Biology, Wake Forest School of Medicine, Winston-Salem, NC, USA; ⁴Department of Microbiology and Immunology, Wake Forest School of Medicine, Winston-Salem, NC, USA; ⁵Department of Neurosurgery, Yale University School of Medicine, New Haven, CT, USA

The difficulty of glioblastoma treatment makes it a good candidate for novel therapies, such as oncolytic viruses. Vesicular stomatitis virus expressing Lassa virus glycoprotein (Lassa-VSV) showed significant promise in animal models using established glioblastoma cell lines. These experiments were to determine the susceptibility of low-passage, patient-derived cell lines to Lassa-VSV oncolysis. Four patient-derived glioblastoma cell lines were infected with Lassa-VSV that expresses green fluorescent protein (GFP) and analyzed by fluorescence microscopy, flow cytometry, and cell viability assays. Cells were also analyzed as tumorspheres containing primarily glioma stem-like cells. Three low-passage, patient-derived cells were further analyzed with RNA sequencing (RNA-seq). Individual cell lines varied somewhat in their levels of viral gene expression and time course of Lassa-VSV-induced cell death, but each was susceptible to Lassa-VSV. Brain Tumor Center of Excellence (BTCOE) 4765 cells had the highest level of expression of interferon-stimulated genes but were most susceptible to Lassa-VSV-induced cell death, indicating that more susceptible cells do not necessarily have lower interferon pathway activation. Cells cultured as tumorspheres and infected with Lassa-VSV also showed variable susceptibility to Lassa-VSV, but BTCOE 4765 cells were least susceptible. Thus, patient-derived brain tumor cells show variable responses to Lassa-VSV infection, but each of the lines was susceptible to VSV oncolysis.

INTRODUCTION

Glioblastoma (GBM) is the most common malignant primary brain tumor in adults. GBM is characterized by rapid and highly invasive growth, histological and genetic heterogeneity, resistance to most chemotherapeutic agents, and a high rate of recurrence.^{1,2} The combination of the highly malignant features of GBM and its location in the brain poses major challenges in therapy.³ There have been small improvements in survival with the addition of treatments with alkylating and antiangiogenic agents. However, the survival benefit is only seen in a subset of patients by only a few months.⁴ Therefore, the

development of novel therapies for the treatment of GBM is a high priority. Among alternative treatment strategies, oncolytic virus therapy holds substantial promise.⁵

The basis of oncolytic virus therapy is the underlying principle that proliferative signaling pathways and antiviral pathways are usually mutually antagonistic.^{6–8} As a result, many cancers develop defects in their antiviral responses, rendering them susceptible to infection with a variety of viruses, many of which are highly cytolytic. In addition to virus-induced cytolysis, a significant aspect of oncolytic virus therapy is stimulation of adaptive immune responses *in vivo* by increasing the tumor immunogenicity via the release of tumor antigens and conversion of the tumor microenvironment to a pro-inflammatory state.⁷

Several oncolytic viruses have been in clinical trials in GBM patients; however, a superior oncolytic virus for the treatment of GBM has yet to be identified. Genetically engineered strains of vesicular stomatitis virus (VSV) are attractive candidate oncolytic viruses for the treatment of many cancers, including GBM. VSV is an enveloped negative-stranded RNA virus of the rhabdovirus family, which causes mild and usually self-limiting disease in livestock.⁹ VSV is one of the most rapidly cytotoxic viruses due to its potent induction of apoptosis and other cell death pathways in infected cancers, including GBM.^{10–12} In addition to direct virus-induced cytolysis, the oncolytic activity of VSV is also due to its pathological effects on tumor vasculature¹³ and its potent ability to elicit both innate and adaptive antitumoral as well as anti-viral immune responses.^{14–17}

The safety of VSV is determined by the fact that it is highly sensitive to interferons (IFNs), preventing spread to normal cells that mount

Received 15 February 2021; accepted 8 June 2021;
<https://doi.org/10.1016/j.omto.2021.06.003>.

⁶Deceased

Correspondence: Douglas S. Lyles, PhD, Department of Biochemistry, Wake Forest School of Medicine, Medical Center Blvd., Winston-Salem, NC 27157, USA.
E-mail: dlyles@wakehealth.edu



IFN-mediated antiviral responses.^{18,19} The application of VSV as an oncolytic virus therapy for GBM, however, has been limited by neurotoxicity in rodent models and non-human primates.^{20–22} Substitution of the envelope glycoprotein of VSV with glycoproteins of different viruses has been shown in several cases to eliminate this neurotoxicity but maintain the oncolytic activity of VSV against GBM.^{21,23–25} Chimeric VSV containing the glycoprotein of Lassa virus (Lassa-VSV) is an example of such a virus with excellent oncolytic activity against GBM in the absence of neurotoxicity, in both immunocompetent and immunodeficient rodent models.²¹

Oncolytic activity of Lassa-VSV has been demonstrated against well-established human GBM cell lines, such as U87 and U118, both *in vitro* and *in vivo*.²¹ The purpose of the experiments presented here was to determine the susceptibility of a broader range of GBM cell types to Lassa-VSV. One of the striking features of GBM tumors is the heterogeneity of GBM cell types both between tumors and also within individual tumors. A widely used classification of GBM subtypes based on transcriptome profiling originally identified four GBM subtypes,²⁶ later revised to three subtypes (mesenchymal, proneural, and classical), based on single-cell RNA sequencing (RNA-seq) and excluding genes overexpressed in non-GBM cells.²⁷ Tumors with high proneural gene expression tend toward a more favorable outcome, whereas mesenchymal signatures relate to poor survival, likely due to the influence of tumor-promoting macrophages and microglial cells.²⁷ These different transcriptional programs serve not only to distinguish between GBM tumors but also to distinguish among GBM cells of different subtypes that have been identified within individual tumors.^{27,28} In addition to the heterogeneity in the major population of GBM cells, GBM tumors contain minor populations of cells with stem-cell like properties.²⁹ These glioma stem-like cells have been shown to evade cytotoxic therapies and continue to fuel tumor growth.^{29–32}

The experiments presented here tested the susceptibility to Lassa-VSV of low passage patient-derived GBM cell lines that vary in their expression of GBM subtype-specific genes and also in glioma stem-like cells derived from these cell lines cultured as tumorspheres. Whereas the individual cell lines varied somewhat in their levels of viral gene expression and time course of Lassa-VSV-induced cell death, each of the cell lines was susceptible to Lassa-VSV. In other cancer types, susceptibility to oncolytic VSVs is often governed by the expression of antiviral IFN-stimulated genes (ISGs, e.g., Carey et al.³³ and Moerdyk-Schauwecker et al.³⁴). Expression of ISG mRNAs was increased following Lassa-VSV infection in the different GBM cell lines, but the level of expression of ISGs was not correlated with Lassa-VSV oncolysis, indicating that ISG expression was not sufficient to prevent virus replication and oncolytic activity.

RESULTS

Expression of GBM subtype signature genes in GBM cell lines

Three GBM cell lines that had been established in the Brain Tumor Center of Excellence (BTCOE) at Wake Forest School of Medicine and validated as derived from the patient's tumor by short tandem

repeat (STR) profiling (BTCOE 4765, BTCOE 4795, and BTCOE 4810)³⁵ were analyzed after a limited number of passages, and a fourth patient-derived cell line, G48, was established earlier.³⁶ Cellular mRNAs were analyzed to determine the extent of variation among the four cell lines in GBM subtype-specific gene-expression signatures, with the understanding that each cell line is likely to contain mixtures of the different gene-expression patterns.²⁷ Gene expression in BTCOE cell lines was determined by RNA-seq and compared with earlier microarray data from G48 cells. The four cell lines differed significantly in their expression of GBM subtype-specific gene signatures. BTCOE 4765 cells expressed highest levels of mRNAs from mesenchymal GBM genes (Figure 1A); G48 cells expressed highest levels from proneural GBM genes (Figure 1B); BTCOE 4795 cells expressed highest levels from classical GBM genes (Figure 1C), and BTCOE 4810 cells expressed intermediate levels of mRNAs from mesenchymal and proneural genes and the lowest levels from classical genes. These data indicate that the four cell lines display a range of gene-expression patterns reflective of the heterogeneity of GBM subtypes.

Susceptibility of GBM cells to Lassa-VSV infection

Susceptibility of GBM cells to Lassa-VSV was determined using a virus that expresses enhanced green fluorescent protein (Lassa-VSV-GFP)³⁷ and analysis by fluorescence microscopy and flow cytometry. BTCOE 4765, BTCOE 4795, BTCOE 4810, and G48 cells were mock infected (control) or infected with Lassa-VSV-GFP at a multiplicity of infection (MOI) of 10 plaque-forming units (PFUs)/cell to establish single-cycle infections, or 0.1 PFU/cell for multiple cycle infections. Living cells were labeled with Hoechst 33342 dye to label nuclei and imaged at 6 and 24 h postinfection by bright-field and fluorescence microscopy (Figure 2). The PFU/cell ratio was based on the virus titer in highly susceptible Vero cells. Thus the assumption that MOI 10 results in single-cycle infections is dependent on the GBM cells being similarly susceptible to Lassa-VSV (see below in Figure 3).

The extent of VSV cytopathic effect (CPE) is apparent in the bright-field images, in which cells that were mostly flat and well spread in the mock-infected control became rounded and shrunken, consistent with the typical morphological changes following induction of apoptosis by VSV.³⁸ Cells infected with Lassa-VSV at MOI 10 showed significant CPE by 6 h postinfection, and cells infected at MOI 0.1 showed extensive CPE by 24 h postinfection. Similarly, most of the cells infected at MOI 10 displayed bright green fluorescent protein (GFP) fluorescence by 6 h postinfection. However, in the case of BTCOE 4765 and BTCOE 4810 cells, much of this GFP fluorescence was lost by 24 h postinfection (Figures 2A and 2C), likely due to membrane rupture as a late effect of VSV-induced apoptosis.³⁸ In the multiple cycle infection at MOI 0.1, there were few cells with bright GFP fluorescence at 6 h postinfection. However, by 24 h postinfection, the virus had spread, resulting in many cells expressing GFP.

Experiments similar to those in Figure 2 were quantified by flow cytometry analysis of GFP fluorescence (Figure 3). BTCOE 4765,

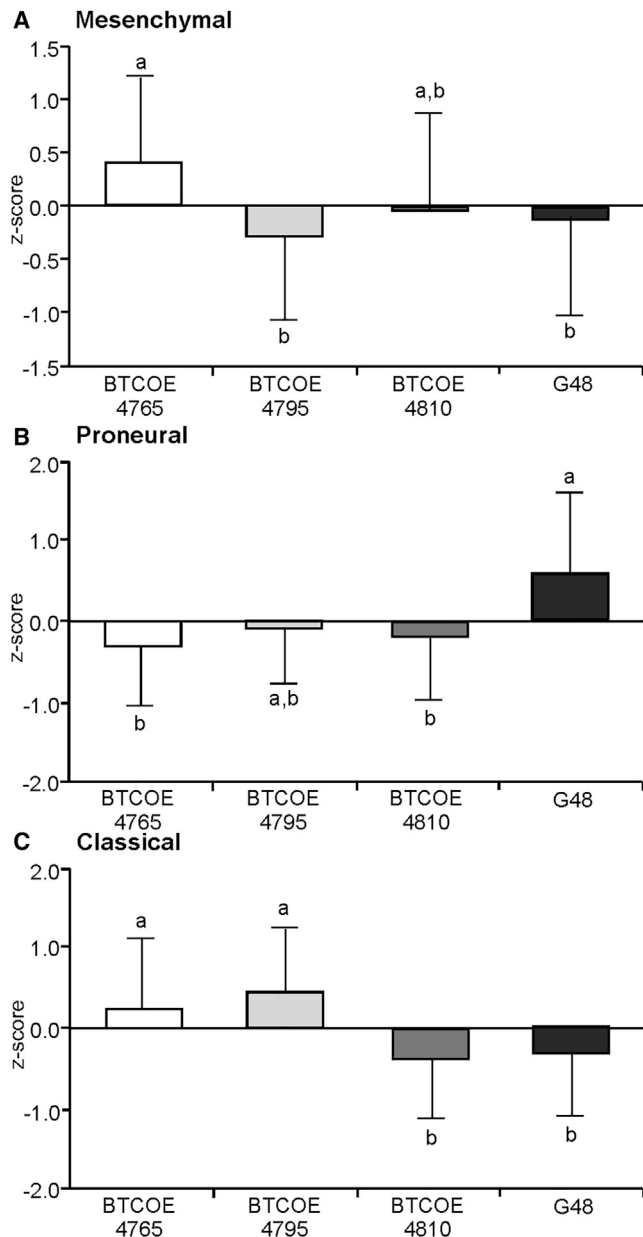


Figure 1. Expression of GBM subtype signature genes in patient-derived GBM cell lines

RNA was extracted from BTCOE 4765, BTCOE 4795, and BTCOE 4810 cells, and mRNA expression was determined by RNA-seq analysis. Data were normalized to total counts and compared to earlier microarray data from G48 cells normalized to total signal intensity. Z scores for GBM subtype-specific signature genes²⁷ expressed in all four cell lines for mesenchymal (A), proneural (B), and classical (C) subtypes were calculated and are shown as mean \pm SD. Cell lines were compared by ANOVA, and groups with $p < 0.05$ are indicated by different letters.

BTCOE 4795, BTCOE 4810, and G48 cells were mock infected or infected with Lassa-VSV-GFP at MOI 10, 1, and 0.1. At 6 or 24 h postinfection, cells were lifted off the dish and fixed in 2% paraformaldehyde,

and the percentage of cells expressing GFP was quantified. Data were gated on intact cells by forward and side scattering, and the control cells were used to establish the gate for GFP-positive cells shown in representative histograms for each cell line in Figures 3A–3D. Figures 3E and 3F show cumulative data for 4 independent experiments as a function of MOI at 6 and 24 h, respectively.

At 6 h postinfection, nearly all of the cells were GFP positive at MOI 10, with the exception of G48 cells (Figure 3, top row), consistent with the infection of BTCOE cells being single-cycle infections. However, the fluorescence intensities did not follow a normal distribution, with a main peak and shoulder (BTCOE 4765 and BTCOE 4795) or two separate peaks (BTCOE 4810 and G48), suggesting heterogeneity in the rate of development of VSV gene expression in these cell lines. The percentage of cells with positive GFP expression showed a dose-dependent increase among MOI 0.1, 1, and 10 across all cell lines (Figures 3E and 3F), with G48 cells having consistently lower percentages of GFP-positive cells.

Time course of loss of viability following infection with Lassa-VSV

The viability of each GBM cell line following Lassa-VSV-GFP infection was assessed using a 3-(4,5-dimethylthiazol-2-yl)-5-(3-carboxymethoxyphenyl)-2-(4-sulfophenyl)-2H-tetrazolium (MTS) assay. Cells were plated in 96-well dishes and then infected with Lassa-VSV-GFP at MOI 10 or 0.1 or mock infected. At 24 h, 48 h, and 72 h, MTS reagent was added, and absorbance was measured and expressed as a percentage of the mock-infected control (Figure 4). BTCOE 4765 and BTCOE 4810 cells rapidly lost viability, with nearly complete loss by 48 h postinfection regardless of whether they were infected at MOI 10 (Figure 4A) or 0.1 (Figure 4B). G48 cells had the slowest loss of viability, and BTCOE 4795 cells had an intermediate time course. Nonetheless, by 72 h, there was little difference in viability among cell lines at MOI 10 and at MOI 0.1. (Only the differences between G48 cells compared to BTCOE 4765 or BTCOE 4810 were statistically significant). Also there was no significant difference in cell viability between infections at MOI 10 and 0.1, except for the 24-h time point of BTCOE 4765 and 48-h time point of G48 cells. The similarity of results at MOI 10 and 0.1 is consistent with a rapid time course of virus spread relative to the time course of cell death.

RNA-seq analysis of IFN pathway activation in GBM cells

VSV is highly susceptible to inhibition by products of ISGs, and virus spread can be controlled by the addition of IFN.²¹ Previous studies in other tumor systems have, in some cases, attributed variable susceptibility to oncolytic VSV to either constitutive expression of ISGs or to ISG expression induced by virus infection.^{33,34} It was hypothesized that the variable susceptibility noted in different GBM cells is due to different levels of ISG expression with more susceptible cells having a lower level of ISG expression.

Expression of mRNAs by the three different low-passage, patient-derived brain tumor cells was determined by RNA-seq analysis.

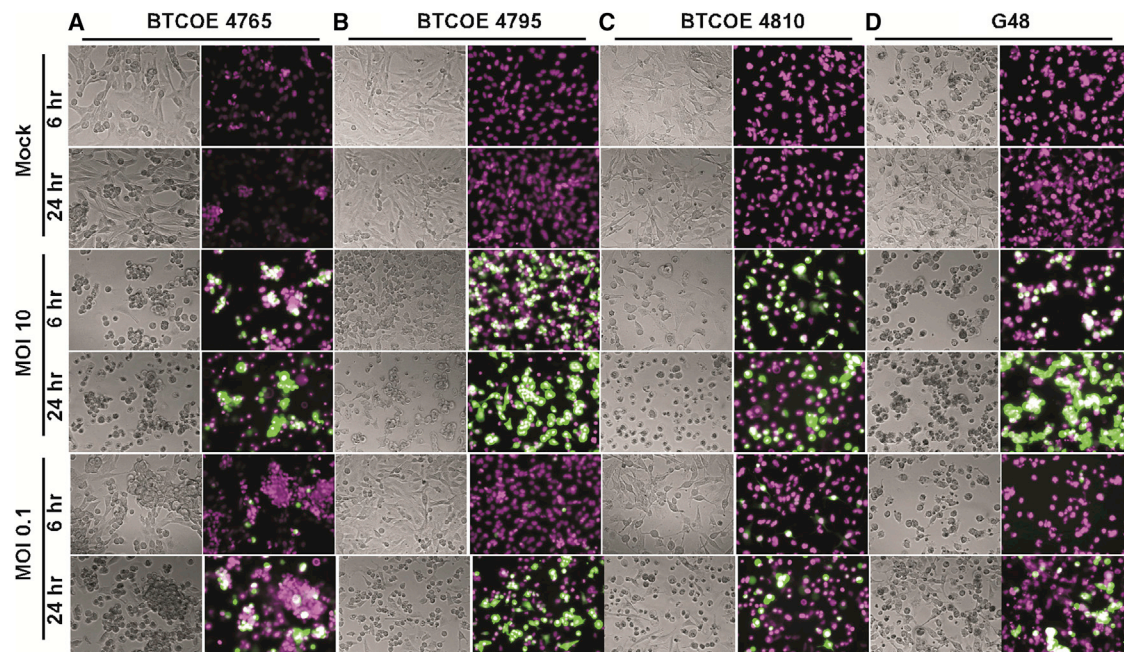


Figure 2. Susceptibility of patient-derived GBM cells to Lassa-VSV in monolayer cultures

BTCOE 4765 (A), BTCOE 4795 (B), BTCOE 4810 (C), and G48 (D) cells were cultured as monolayers and mock infected or infected with Lassa-VSV, which expresses GFP at MOI 10 and 0.1. The cells were stained with Hoechst 33342 to identify the nuclei and were imaged as live cells with bright-field and fluorescence microscopy after 6 and 24 h infection. Expression of GFP indicated by green identified Lassa-VSV-infected cells, and nuclei are indicated by magenta.

BTCOE 4765, 4795, and 4810 were either mock infected or infected with Lassa-VSV at MOI 10. At 6 h postinfection, RNA was isolated, and mRNA sequences were determined and analyzed by gene set enrichment analysis (GSEA). Table S1 shows the mRNA expression levels used in this analysis. Pairwise comparison of mRNA levels in each cell line was used to generate an ordered dataset of genes for each pair based on signal-to-noise ratio of their differential expression. The results were analyzed for differential expression of curated gene sets from the Molecular Signatures Database version (v.)6.2 (Broad Institute). Table S1 contains examples of immune or growth-regulatory pathways that were differentially expressed. Table S2 contains results for the Hallmark_Interferon_Alpha_Response gene set, which comprises 97 genes related to IFN signaling. The pairwise comparisons among BTCOE cell lines showed that expression of genes in the gene set occurred in the order BTCOE 4765 > BTCOE 4810 > BTCOE 4795 for both mock- and Lassa-VSV-infected cells. Figure 5 shows mRNA expression levels for the top 10 genes that differ in this analysis between BTCOE 4765 and BTCOE 4795 mock-infected cells. As expected from their method of selection, expression of most of these genes reflected the order in the gene set as a whole, BTCOE 4765 > BTCOE 4810 > BTCOE 4795. Notable exceptions were the high level of interleukin (IL)-15 mRNA expression (Figure 5F) and the low levels of expression of IFITM2, HELZ2, IFITM3, and PSME2 mRNAs (Figures 5D, 5E, 5H, and 5I) in BTCOE 4810 cells. Also notable were the modest and often not statistically significant differences between mock- and Lassa-VSV-infected cells for most of these genes (with the exception of IL-15 and ISG15 in

BTCOE 4765 cells; Figures 5F and 5J). This result is consistent with a limited ability to mount an antiviral response against Lassa-VSV in these cells.

BTCOE 4765 cells were among the most susceptible of the cell lines in terms of the percent of cells infected (Figure 3E) and the induction of cell death (Figure 4). However, they expressed the highest levels IFN- α pathway genes. Overall, the RNA-seq analysis is inconsistent with the hypothesis that the variable susceptibility to Lassa-VSV is due exclusively to IFN pathway gene expression.

Susceptibility to Lassa-VSV infection of glioma stem-like cells in tumorspheres

Glioma stem-like cells often have greater resistance to radiation and chemotherapeutic agents.^{30–32} This raises the question of the degree of susceptibility of glioma stem-like cells to Lassa-VSV. Cells were cultured under tumorsphere-forming conditions in order to enrich the population of glioma stem-like cells. The tumorspheres were distributed as evenly as possible and infected with 10^5 , 10^6 , and 10^7 PFU of Lassa-VSV-GFP and incubated for 24 h. Tumorspheres were analyzed by confocal fluorescence microscopy. Figure 6 shows representative slices from z stacks of tumorsphere images.

Tumorspheres showed a dose-dependent increase in GFP signal; a higher GFP signal was observed when infected with a higher PFU of Lassa-VSV. It is difficult to quantify the MOI due to the spherical structure of tumorspheres, but there is a qualitative difference in the

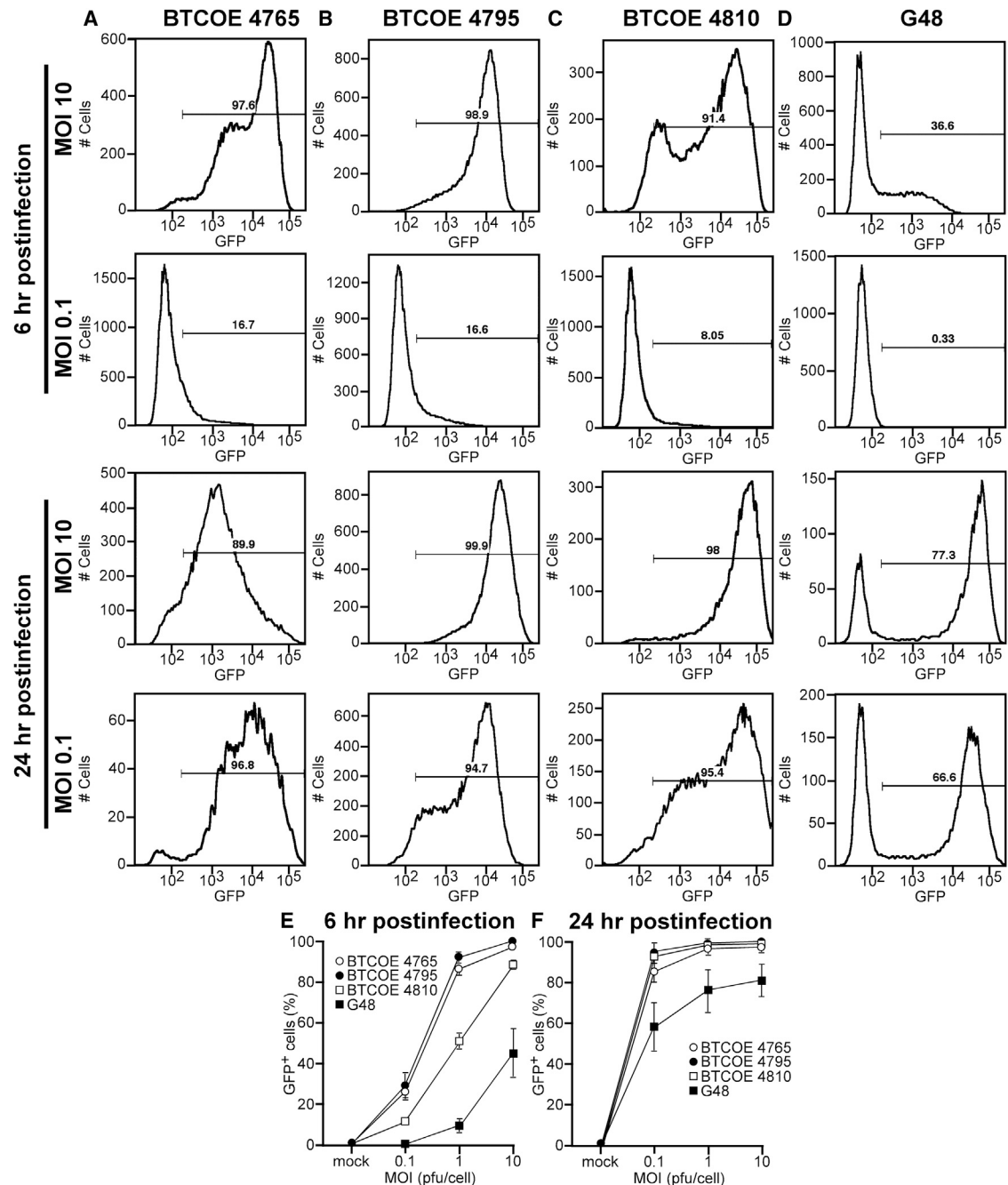


Figure 3. Flow cytometry quantification of Lassa-VSV infection of GBM cells

BTCOE 4765 (A), BTCOE 4795 (B), BTCOE 4810 (C), or G48 (D) GBM cells were infected with Lassa-VSV, which expresses GFP at MOI 0.1, 1, or 10 for 6 and 24 h. Cells were detached from the dish and fixed with 2% paraformaldehyde, and GFP expression was analyzed by flow cytometry. Data were gated on intact cells by forward and side scattering, and gates for positive GFP expression were determined from mock-infected controls. The histograms shown in columns (A–D) are from a representative experiment after infection at MOI 10 and 0.1. The graphs shown in (E) and (F) show the mean percentage of cells with GFP expression \pm SEM from 4 experiments at MOI 0.1, 1, and 10 for 6 and 24 h infection.

number of GFP-positive cells when compared to monolayer cultures, particularly at low virus doses, indicating that spread of virus through the tumorspheres occurred slowly.

Flow cytometry of GFP expression and markers for glioma stem-like cells, CD44 and Nestin, was performed in order to quantify the level of infectivity of glioma stem-like cells in tumorspheres. [Figure 7](#)

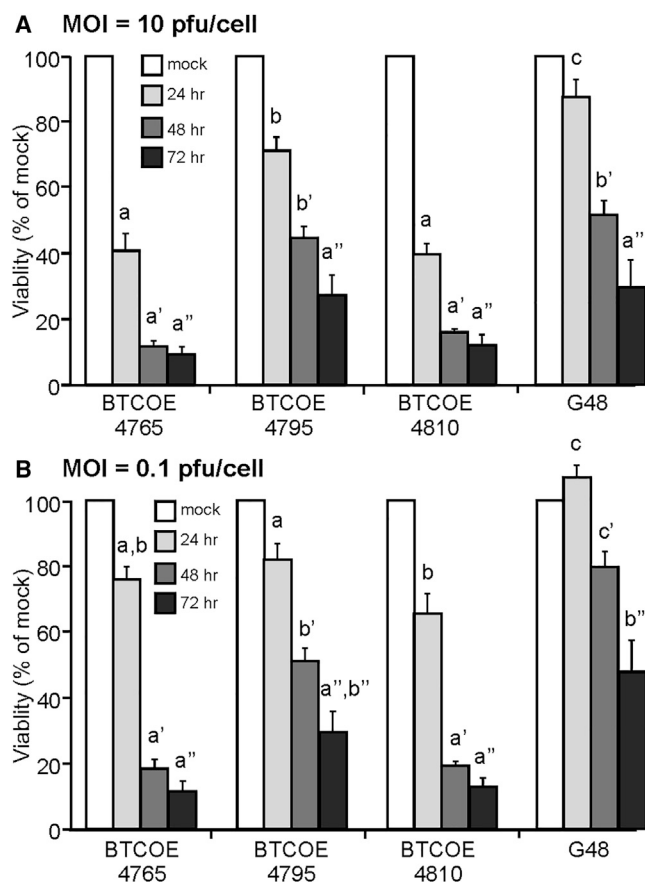


Figure 4. Analysis of viability of patient-derived brain tumor cells infected with Lassa-VSV

The indicated GBM cells were mock infected or infected with Lassa-VSV at MOI 10 (A) and 0.1 (B). MTS assays for viability were performed after 24, 48, and 72 h, and data are expressed as percent of mock-infected controls. The graphs show the mean \pm SEM of 9 experiments for 24- and 48-h time points and 5 experiments for the 72-h time point. Statistical analysis was performed by ANOVA of the four cell lines at 24 h (a, b, and c), 48 h (a', b', and c'), and 72 h (a'' and b''). Groups with $p < 0.05$ are indicated by different letters.

shows the distribution of cells that were mock infected or infected with Lassa-VSV-GFP at 10^7 PFU from a representative experiment (Figures 7A–7D) and cumulative data from multiple experiments at the three different virus doses (Figures 7E and 7F). The majority of cells in mock-infected control tumorspheres was marker positive, ranging from approximately 50% to >90%, depending on the cell type and marker. There was a greater fraction of cells expressing high levels of GFP for both CD44- and Nestin-positive cell populations compared to CD44- and Nestin-negative populations (Figures 7A–7D). When individual cell lines are compared, BTCOE 4810 and BTCOE 4795 cells had the highest proportion of cells positive for glioma stem-like markers that were infected with Lassa-VSV-GFP (Figures 7E and 7F). This was consistently seen at the three different doses and for both CD44- and Nestin-positive cells. G48 cells had an intermediate level of glioma stem-like cell susceptibility

to Lassa-VSV-GFP infection, and BTCOE 4765 glioma stem-like cells were the least susceptible to Lassa-VSVGFP infection. This order of susceptibility (BTCOE 4810 \approx BTCOE 4795 > G48 > BTCOE 4765) differed from that of cells grown in monolayer cultures (Figure 3E; BTCOE 4765 \approx BTCOE 4795 > BTCOE 4810 > G48).

DISCUSSION

The data presented here show the extent to which patient-derived GBM cells differ in their responses to infection with Lassa-VSV. Among the responses that are important for oncolytic activity analyzed here are the following: (1) the ability of cells to resist virus infection in a single-cycle infection, (2) the ability to inhibit spread of virus in a multiple cycle infection, (3) the extent and time course of cell death induced by virus, and (4) the ability to express antiviral ISGs. Lassa-VSV was able to infect all four of the cell lines analyzed here to different extents in a single-cycle infection and was able to spread throughout the cultures in a multiple cycle infection, so that by 24 h postinfection, nearly all of the cells were infected (Figures 2 and 3), and by 72 h postinfection, nearly all of the cells were nonviable (Figure 4). The GBM cells were able to express some ISG mRNAs in response to virus infection (Figure 5; Table S2), but this response was not effective in preventing viral oncolysis. Thus, none of the GBM cells displayed the resistance to VSV infection that has been observed in a subset of cell lines from other tumor types such as prostate cancer and pancreatic cancer that express high levels of ISGs nor have the well-established human GBM cell lines analyzed previously displayed such resistance. In the case of Lassa-VSV infection of tumorspheres, however, the multiple cycle infection proceeded much more slowly so that only at the highest dose of virus was a substantial fraction of cells infected with Lassa-VSV-GFP by 24 h postinfection (Figures 5 and 6). Nonetheless, Nestin- or CD44-positive glioma stem-like cells were more susceptible to Lassa-VSV infection than marker-negative cells in tumorspheres (Figures 6A–6D), suggesting that Lassa-VSV will also have oncolytic activity against stem-like cells in GBM tumors.

Despite the observation that GBM cells were generally susceptible to Lassa-VSV infection, there was substantial diversity in their responses to Lassa-VSV infection. To illustrate this diversity, data from each of the experimental series were subjected to principal component (PC) analysis (PCA) to determine the major sources of variability among cell lines (Table S3). The results of these analyses are summarized in Table 1. For example, BTCOE 4795 cells were among the most susceptible to Lassa-VSV-GFP infection in terms of the percentage of cells infected at different virus doses in monolayer cultures (Figures 3E and 3F; Table 1) but were among the least sensitive to Lassa-VSV-induced cell death, as indicated by the loss of cell viability in the MTS assay (Figure 4; Table 1), as well as the morphological changes associated with VSV-induced CPE and the loss of GFP upon cell lysis as a late stage in VSV-induced CPE (Figure 2). In contrast to BTCOE 4795 cells, BTCOE 4810 and 4765 were the most sensitive to Lassa-VSV-induced cell death (Figure 4; Table 1), despite expressing lower levels of virus-encoded GFP (Figure 3; Table 1). The previously established cell line G48 was the least susceptible to

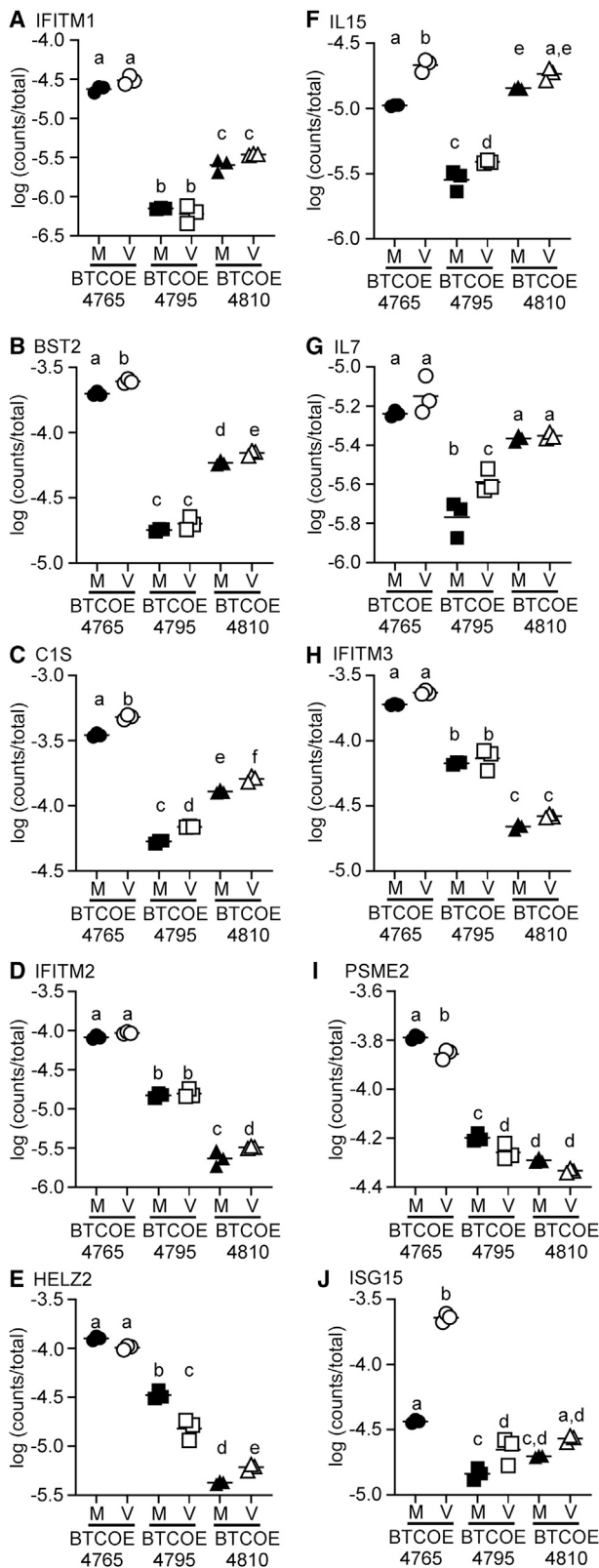


Figure 5. Expression of interferon pathway genes in patient-derived GBM cell lines

BTCOE 4765, BTCOE 4795, and BTCOE 4810 cells were mock infected (M) or infected with Lassa-VSV (V) at MOI 10. RNA was extracted at 6 h postinfection, and mRNA expression was determined by RNA-seq analysis. Data were normalized to total counts and analyzed by gene set enrichment analysis. Expression levels of mRNAs for the top 10 differentially expressed genes between BTCOE 4765 and BTCOE 4795 mock-infected cells in the Hallmark_Interferon_Alpha_Response gene set are shown from three independent experiments together with their means [IFITM1 (A), BST2(B), C1S (C), IFITM2 (D), HELZ2 (E), IL15 (F), IL7 (G), IFITM3 (H), PSME2 (I), and ISG15 (J)]. Cell lines were compared by ANOVA, and groups that were significantly different at $p < 0.05$ are indicated by different letters.

Lassa-VSV both in terms of GFP expression and loss of cell viability (Figures 3 and 4; Table 1).

It is well established that VSV induces cell death primarily by induction of apoptosis in infected cells.³⁹ The induction of apoptosis occurs by multiple mechanisms. One mechanism is due to the inhibition of host gene expression by the viral matrix (M) protein. Another involves induction of host gene expression, which includes a variety of pro-apoptotic gene products. This process is most apparent in the case of M protein mutant viruses that are defective in the inhibition of host gene expression. Also, different cell types differ in their responses to these two mechanisms.^{38,39} Since Lassa-VSV has a wild-type M protein, both mechanisms are likely to contribute to cell death. Also, VSV activates other cell death pathways in addition to apoptosis, which are apparent in cells in which apoptosis has been inhibited.¹¹ The differential activation of these multiple cell death pathways is likely to account for the differences in the time courses of cell death among GBM cells.

There was also significant diversity in the expression of antiviral ISGs among the cells analyzed here, but ISG expression did not correlate with their susceptibility to Lassa-VSV infection (Figure 5; Table 1). ISG expression in cancer cells can occur both constitutively, due to constitutive activation of antiviral pathways,^{33,34,40} and/or expression can be induced in response to virus infection or to treatment with IFNs.⁴¹ Constitutive ISG expression tends to be important for inhibition of early events in virus infection,³³ and induced expression is important for inhibition of later events and virus spread.⁴¹ BTCOE 4765 cells expressed the highest levels of ISG mRNAs, both constitutively and induced by virus infection (Figure 5; Table 1), but were among the most sensitive to virus infection, at least in monolayer cultures. Also notable were the modest differences in ISG expression between mock- and Lassa-VSV-infected cells (Figure 5). This is also clear in the PCA (Table S3; graph in sheet “ISG mRNA”), in which for each cell line, mock- and Lassa-VSV-infected cells cluster closely together. This likely reflects a combination of the suppression of antiviral pathways in GBM cells and the inhibitory effect of the wild-type VSV M protein on cellular gene expression.⁹

The results presented here raise the question of whether there is a correlation between the expression of GBM subtype-specific genes and the response to oncolytic viruses. Clearly, the limited number of cell lines

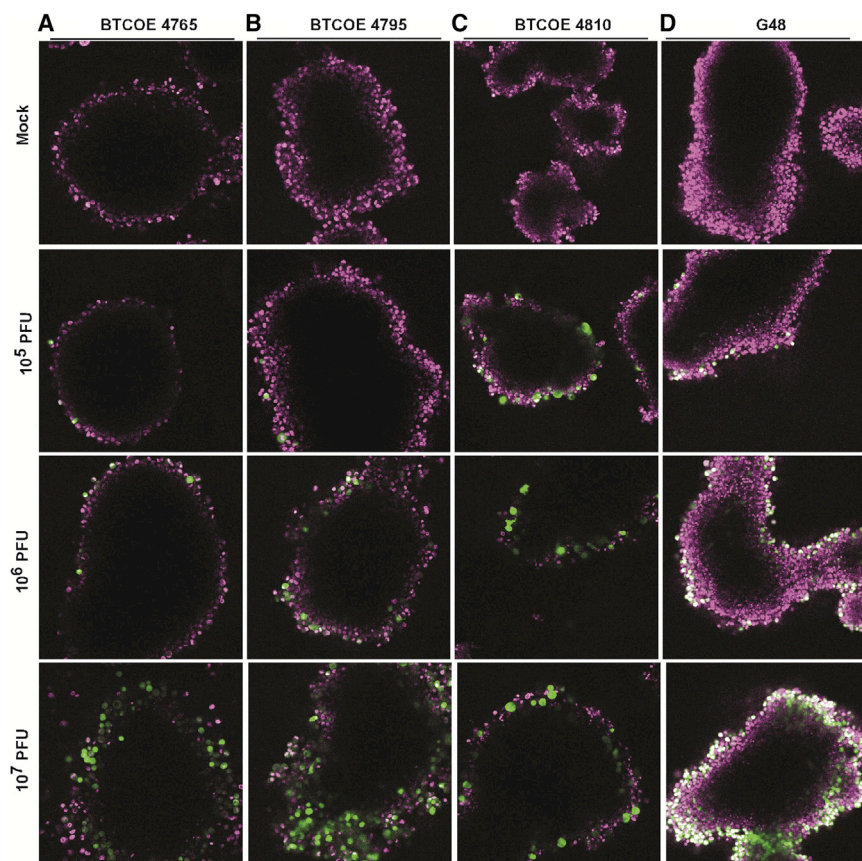


Figure 6. Susceptibility of tumorspheres grown from patient-derived brain tumor cells to Lassa-VSV infection

BTCOE 4765 (A), BTCOE 4795 (B), BTCOE 4810 (C), or G48 (D) GBM cells were cultured under conditions to form tumorspheres. The tumorspheres were mock infected or infected with Lassa-VSV that expresses GFP at 10^5 , 10^6 , and 10^7 PFU. After 24 h infection, the cells were stained with Hoechst 33342 to identify nuclei and imaged with confocal microscopy. Images shown here are representative images from z stacks. Expression of GFP indicated by green shows Lassa-VSV-infected cells, and nuclei are labeled with magenta.

Patient-derived brain tumor cells

Patient-derived brain tumor cells were obtained from the BTCOE at Wake Forest School of Medicine. BTCOE 4765, BTCOE 4795, and BTCOE 4810 cells are low passage (between 40 and 70 passages) and have been validated as derived from the patient's tumor by STR profiling,³⁵ and a fourth patient-derived cell line, G48, was established earlier.³⁶ Cells were maintained in RPMI medium (Thermo Fisher Scientific, Gibco, Waltham, MA, USA) with 10% fetal calf serum, 1% glucose, 1% sodium pyruvate, and L-glutamine.

Generation of tumorspheres

Cells were detached from culture dishes using trypsin and were resuspended in tumorsphere medium, which lacks fetal calf serum. Tumor-

sphere medium is composed of neurobasal medium (Thermo Fisher Scientific, Gibco, Waltham, MA, USA) with 1:20 penicillin/streptomycin, 1:20 glutamine, 1% N2 100× supplement (manufacturer number 17502048; Thermo Fisher Scientific, Gibco, Waltham, MA, USA), 2% B27 50× supplement (manufacturer number 17504044; Thermo Fisher Scientific, Gibco, Waltham, MA, USA), 100 μ L fibroblast growth factor (FGF; 0.02 μ g/ μ L [10 μ g dissolved in 500 μ L sterile water], manufacturer number PHG0024; Thermo Fisher Scientific, Gibco, Waltham, MA, USA), and 20 μ L epidermal growth factor (EGF; 0.2 μ g/ μ L [100 μ g dissolved in 500 μ L sterile PBS], manufacturer number PHG0311; Thermo Fisher Scientific, Gibco, Waltham, MA, USA) for 100 mL stock media. 1×10^6 cells were added to 5 mL of tumorsphere media in 60 mm \times 15 mm ultra-low binding culture dishes (Corning, Tewksbury, MA, USA) and incubated at 37°C with 5% CO₂. On culture day 4, the tumorspheres were placed in a 15-cc tube, centrifuged, and placed back in the same culture dish with fresh tumorsphere media. Tumorspheres were analyzed for susceptibility to Lassa-VSV infection on days 7–10.

MATERIALS AND METHODS

Generation of Lassa-VSV stock

Lassa-VSV has a substitution of the Lassa virus GPC gene for the VSV G gene and a separate transcription unit encoding enhanced GFP.³⁷ Stocks were prepared in Vero cells infected at an MOI of 0.01 PFU/cell. The infected Vero cells were cultured at 37°C with 5% CO₂ for 36 h until CPE was noted. The culture media were collected and centrifuged at 2,000 rpm for 15 min, and the supernatant was collected and frozen at -80°C . Titers were determined by plaque assay on Vero cells, which gave a titer of 2.2×10^8 PFUs/mL.

analyzed here cannot answer this question. However, evidence from other tumor types suggests that responses to oncolytic viruses may be independent of other genetic alterations. For example, in a transgenic mouse model of prostate cancer, both VSV-sensitive and VSV-resistant cells arise from a single genetic lesion (prostate-specific deletion of *Pten*) and can be altered by changes in the tumor microenvironment, such as hormone deprivation.⁴² Other evidence suggests that responses to oncolytic virus are governed by responses to tumor microenvironments that are maintained in cancer cells by epigenetic mechanisms.^{43–45} A striking feature of GBM is the heterogeneity of tumor microenvironments, and it is likely that this factor may play a role in the observed diversity of responses to oncolytic responses to Lassa-VSV described here.

Lassa-VSV infection in monolayer for fluorescence microscopy

Cells were disassociated from culture dishes, resuspended in fresh brain tumor culture media, and seeded in 6-well dishes with 1×10^6 cells per well. The following day, cells were infected with

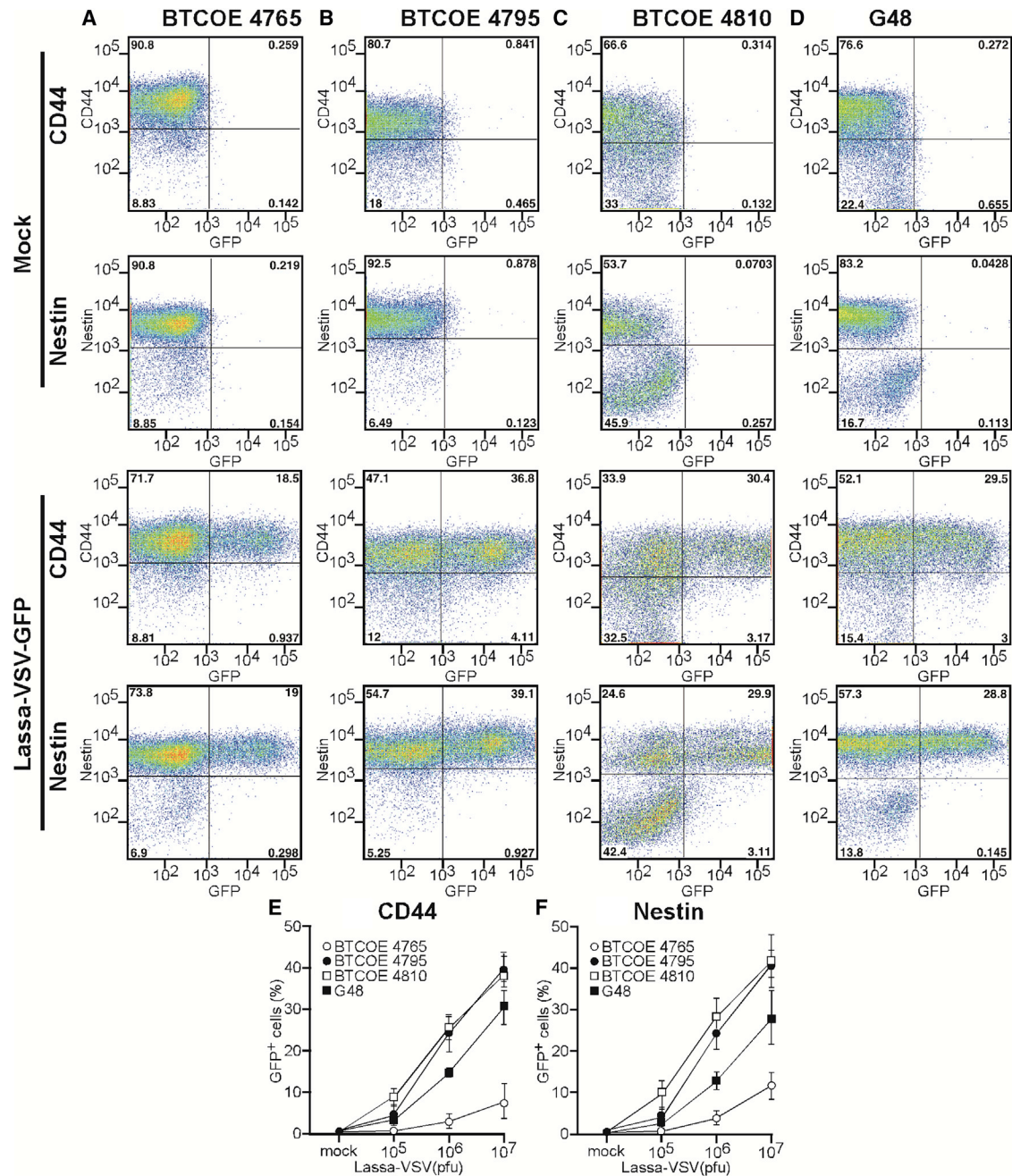


Figure 7. Susceptibility of glioma stem-like cells to Lassa-VSV infection

BTCE 4765 (A), BTCE 4795 (B), BTCE 4810 (C), or G48 (D) brain tumor cells grown as tumorspheres were mock infected (control) or infected with Lassa-VSV that expresses GFP at 10^5 , 10^6 , and 10^7 PFU. After 24 h infection, cells were dissociated, surface labeled for CD44, and then permeabilized and labeled for Nestin. Flow cytometry was performed with columns (A–D) indicating color dot plots from a representative experiment with 10^7 PFU. (E) and (F) show the fraction of marker-positive cells that are also GFP positive (i.e., infected with Lassa-VSV) at three different doses. Data shown are means \pm SEM from 4 experiments for infected cells and mock-infected control from 2 experiments.

Lassa-VSV at MOIs of 0.1, 1, or 10 PFU/cell or were mock infected as negative controls. The cells were labeled with Hoechst 33342 stain (Biotium, Fremont, CA, USA) to label nuclei and imaged

with a Nikon Eclipse TE300 fluorescence microscope (Nikon, Melville, NY, USA) at 6 h and 24 h postinfection without being fixed.

Table 1. Summary of principal component analyses of data on Lassa-VSV infection of patient-derived GBM cells^a

Experimental series	Principal component	Percent of total variance	Major correlations with original variables ^b	Rank order of cell line coordinates ^c
Flow cytometry (Figures 3E and 3F)	PC1	77%	6 h-MOI 1	4795 > 4765 > 4810 > G48
			6 h MOI 10	
			24 h-MOI 0.1	
Cell viability (Figure 4)	PC1	78%	48 h-MOI 0.1	4810 > 4765 > 4795 > G48
			24 h-MOI 10	
			48 h-MOI 10	
			24 h-MOI 0.1	
ISG mRNA expression (Figure 5)	PC1	54%	IFITM1	4765 > 4795 ≈ 4810
			IFITM2	
			HELZ2	
	PC2	30%	IFITM2	4795 > 4765 > 4810
			HELZ2	
GBM stem-like cells flow cytometry (Figures 7E and 7F)	PC1	81%	IL-15	4810 > 4765 > 4795
			IFITM1	
			10 ⁷ PFU-CD44	
			10 ⁷ PFU-Nestin	
			10 ⁶ PFU-CD44	
			10 ⁶ PFU-Nestin	4810 > 4795 > G48 > 4765

^aSummaries of principal component (PC)s that account for >75% of total variance from analyses in Table S3.

^bVariables in which correlations with the PC are 0.4 or greater, regardless of whether the correlation is positive or negative.

^cRank order of cell line coordinates on PCs based on magnitude of the biological effect, regardless of whether the coordinates are positive or negative.

Lassa-VSV infection in tumorspheres for confocal microscopy

Eight-well chambered coverslips (Thermo Fisher Scientific, Waltham, MA, USA) were coated with 1 mL Sigmacote (Millipore Sigma, Darmstadt, Germany), washed with 1 mL sterile water three times, and allowed to dry. 500 µL of the suspended tumorspheres was aliquoted to each well and infected with Lassa-VSV at 10⁵, 10⁶, or 10⁷ PFU per chamber or was mock infected as a negative control. Following a 24-h incubation period, Hoechst 33342 stain (Biotium, Fremont, CA, USA) was applied to label nuclei, and cells were imaged with a Nikon Eclipse Ti confocal microscope (Nikon, Melville, NY, USA) without being fixed.

MTS viability assay

Cells were seeded into 96-well plates at 1 × 10⁴ cells per well. The cells were allowed to incubate overnight followed by virus infection the following day. Cells were infected in triplicate with Lassa-VSV at MOI 0.1 and 10 and mock infected as negative controls. At 24, 48, or 72 h, 20 µL of MTS reagent (CellTiter 96; Promega, Madison, WI, USA) was added to each well and allowed to incubate 1–4 h according to the manufacturer's instruction. Once incubation was complete, absorbance was measured at 490 nm on a POLARstar Omega plate reader (BMG Labtech, Cary, NC, USA).

Flow cytometry analysis of monolayer Lassa-VSV infection

Cells were seeded at 1 × 10⁶ cells per well in 6-well dishes, allowed to incubate overnight, and were infected with Lassa-VSV at MOI 0.1, 1,

and 10 or mock infected as a control. After 6 or 24 h, cells were washed with PBS and lifted off the wells with trypsin. After centrifugation, cells were fixed with 2% paraformaldehyde. Flow cytometry was performed on an LSRFortessa X-20 instrument (BD Biosciences, San Jose, CA, USA).

Flow cytometry analysis of tumorspheres labeled with antibodies to markers for tumor stem-like cells

Tumorspheres were cultured and infected as described. The tumorspheres were then dissociated with Accumax (Sigma-Aldrich, Darmstadt, Germany) by gentle agitation and incubation at 37°C. Once the tumorspheres were adequately dissociated, cells were resuspended in PBS, and 200 µL aliquots were placed in a 96-well plate. Cells were stained with anti-human CD44 antibody with allophycocyanin (APC) fluorophore (mouse immunoglobulin G1 [IgG1], kappa isotype; BioLegend, San Diego, CA, USA). Cells were permeabilized using Cytotfix/Cytoperm (BD Pharmingen, San Jose, CA, USA) according to the manufacturer's instructions. Cells were then stained with anti-mouse Nestin antibody with PerCP-Cy5.5 fluorophore (mouse IgG1, kappa isotype; BD Pharmingen, San Jose, CA, USA). Flow cytometry was performed on LSRFortessa X-20 (BD Biosciences, San Jose, CA, USA).

RNA-seq analysis

BTCOE 4765, 4795, and 4810 cells in monolayer cultures were either mock infected or infected with Lassa-VSV at MOI 10. At

6 h postinfection, cells were lifted off the plate and pelleted. RNA was extracted from three independent samples of each cell population using the RNeasy kit (QIAGEN, Germantown, MD, USA). Total RNA was used to prepare cDNA libraries using the Illumina TruSeq Stranded Total RNA with Ribo-Zero Gold Preparation kit (Illumina, San Diego, CA, USA). RNA integrity number (RIN) values for the samples ranged from 9.7 to 10. Briefly, 750 ng of total RNA was rRNA depleted, followed by enzymatic fragmentation, reverse-transcription, and double-stranded cDNA purification using AMPure XP magnetic beads (Beckman Coulter, Brea, CA, USA). The cDNA was end repaired, 3' adenylated, with Illumina sequencing adaptors ligated onto the fragment ends, and the stranded libraries were pre-amplified with PCR. The library size distribution was validated and quality inspected using an Agilent 2100 Bioanalyzer. The quantity of each cDNA library was measured using the Qubit 3.0 (Thermo Fisher Scientific, USA). The libraries were pooled and sequenced to a target read depth of 30 M reads per library using single-end 76 cycle sequencing with the High Output 75-cycle kit (Illumina) on the Illumina NextSeq 500. Genome alignment was performed using in-house R scripts and the Spliced Transcripts Alignment to a Reference (STAR) sequence aligner, and gene counts for mapped reads were determined. This work was performed by the Cancer Genomics Shared Resource and the Bioinformatics Shared Resource of the Wake Forest Baptist Comprehensive Cancer Center.

Statistical analysis

The RNA-seq raw count data were filtered using Gene Cluster 3.0 (Miyano Laboratory, University of Tokyo, Tokyo, Japan) to eliminate genes with less than 50 counts in all samples. Counts were normalized by dividing by total counts in each sample. GSEA (Broad Institute, Massachusetts Institute of Technology, Cambridge, MA, USA, and University of California, San Diego, La Jolla, CA, USA) was performed on pairwise comparisons of the cell lines using the Hallmark Gene Set library. Statistics were determined by 1,000 permutations of the gene sets.^{46,47} Gene sets with nominal p values of ≤ 0.05 and false discovery rate (FDR) q values ≤ 0.25 were considered significantly different between cell lines. For the data in Figure 5, expression levels of mRNAs for the top 10 differentially expressed genes between BTCOE 4765 and BTCOE 4795 mock-infected cells in the Hallmark_Interferon_Alpha_Response gene set (Molecular Signatures Database v.6.2; Broad Institute) were log transformed, then compared by one-way ANOVA, followed by Tukey's multiple comparisons test using GraphPad Prism v.8.2.1 software for Windows (GraphPad Software, San Diego, CA, USA; <https://www.graphpad.com/>).

Expression of GBM subtype signature genes in BTCOE 4765, 4795, and 4810 cells from RNA-seq data was compared to previous microarray data from G48 cells. RNA-seq data for each gene were normalized to total counts and expressed as counts per million reads. Similarly, signal intensity data from microarray analysis were normalized to total intensity and expressed as intensity per million intensity units. GBM signature genes expressed in all four cell lines were identified

using MATLAB scripts; their expression levels were converted to Z scores, and the distributions of Z scores among these genes were compared by one-way ANOVA, followed by Tukey's multiple comparisons test using GraphPad Prism v.8.2.1.

MTS and flow cytometry data were analyzed by one-way ANOVA, followed by Tukey's multiple comparisons test using GraphPad Prism v.8.2.1 for Windows.

Quantitative data from each of the experimental series (Figures 3E and 3F; Figure 4; Figure 5; and Figures 7E and 7F) were analyzed for PCs using Cluster 3.0 for Mac OS X (C Clustering Library 1.56). ISG mRNA expression data were log transformed prior to PCA.

SUPPLEMENTAL INFORMATION

Supplemental information can be found online at <https://doi.org/10.1016/j.omto.2021.06.003>.

ACKNOWLEDGMENTS

The authors deeply mourn the death of coauthor Dr. Anthony van den Pol on October 28, 2020.⁴⁸ This study was supported by National Institutes of Health (NIH) grant R01 AI105012 (to D.S.L.), pilot funds from the Brain Tumor Center of Excellence, Wake Forest School of Medicine, and an Andrew T. Parsa Research Fellowship Award from the Neurosurgery Research & Education Foundation (to T.E.K.). We also acknowledge the support of the Bioinformatics, Cancer Genomics, Cell Engineering, and Flow Cytometry Shared Resources of the Wake Forest Baptist Comprehensive Cancer Center supported by NIH grant P30 CA012197.

AUTHOR CONTRIBUTIONS

T.E.K., S.P., and K.Z. performed experiments. D.M.H. and W.D. generated the cell lines and originally suggested the analysis of viral susceptibility and provided training. D.A.O., A.N.v.d.P., W.D., and D.S.L. designed experiments and analyzed data. T.E.K. and D.S.L. wrote the first drafts of the manuscript, and all authors contributed to manuscript revisions.

DECLARATION OF INTERESTS

The authors declare no competing interests.

REFERENCES

- Ostrom, Q.T., Gittleman, H., Farah, P., Ondracek, A., Chen, Y., Wolinsky, Y., Stroup, N.E., Kruchko, C., and Barnholtz-Sloan, J.S. (2013). CBTRUS statistical report: Primary brain and central nervous system tumors diagnosed in the United States in 2006-2010. *Neuro-oncol.* 15 (Suppl 2), ii1-ii56.
- Kumthekar, P.U., Macrie, B.D., Singh, S.K., Kaur, G., Chandler, J.P., and Sejjal, S.V. (2014). A review of management strategies of malignant gliomas in the elderly population. *Am. J. Cancer Res.* 4, 436-444.
- Taylor, O.G., Brzozowski, J.S., and Skelding, K.A. (2019). Glioblastoma Multiforme: An Overview of Emerging Therapeutic Targets. *Front. Oncol.* 9, 963.
- Van Meir, E.G., Hadjipanayis, C.G., Norden, A.D., Shu, H.K., Wen, P.Y., and Olson, J.J. (2010). Exciting new advances in neuro-oncology: the avenue to a cure for malignant glioma. *CA Cancer J. Clin.* 60, 166-193.

5. Martikainen, M., and Essand, M. (2019). Virus-Based Immunotherapy of Glioblastoma. *Cancers (Basel)* 11, 186.
6. Critchley-Thorne, R.J., Simons, D.L., Yan, N., Miyahira, A.K., Dirbas, F.M., Johnson, D.L., Swetter, S.M., Carlson, R.W., Fisher, G.A., Koong, A., et al. (2009). Impaired interferon signaling is a common immune defect in human cancer. *Proc. Natl. Acad. Sci. USA* 106, 9010–9015.
7. Lichty, B.D., Breitbach, C.J., Stojdl, D.F., and Bell, J.C. (2014). Going viral with cancer immunotherapy. *Nat. Rev. Cancer* 14, 559–567.
8. Russell, S.J., Peng, K.-W., and Bell, J.C. (2012). Oncolytic virotherapy. *Nat. Biotechnol.* 30, 658–670.
9. Lyles, D.S., Kuzman, I.V., and Rupprecht, C.E. (2013). Rhabdoviridae. In *Fields Virology*, Sixth Edition, D.M. Knipe and P.M. Howley, eds. (Philadelphia: Lippincott Williams & Wilkins), pp. 885–922.
10. Balachandran, S., Porosnicu, M., and Barber, G.N. (2001). Oncolytic activity of vesicular stomatitis virus is effective against tumors exhibiting aberrant p53, Ras, or myc function and involves the induction of apoptosis. *J. Virol.* 75, 3474–3479.
11. Cary, Z.D., Willingham, M.C., and Lyles, D.S. (2011). Oncolytic vesicular stomatitis virus induces apoptosis in U87 glioblastoma cells by a type II death receptor mechanism and induces cell death and tumor clearance in vivo. *J. Virol.* 85, 5708–5717.
12. Wollmann, G., Tattersall, P., and van den Pol, A.N. (2005). Targeting human glioblastoma cells: comparison of nine viruses with oncolytic potential. *J. Virol.* 79, 6005–6022.
13. Breitbach, C.J., De Silva, N.S., Falls, T.J., Aladl, U., Evgin, L., Paterson, J., Sun, Y.Y., Roy, D.G., Rintoul, J.L., Daneshmand, M., et al. (2011). Targeting tumor vasculature with an oncolytic virus. *Mol. Ther.* 19, 886–894.
14. Galivo, F., Diaz, R.M., Wongthida, P., Thompson, J., Kottke, T., Barber, G., Melcher, A., and Vile, R. (2010). Single-cycle viral gene expression, rather than progressive replication and oncolysis, is required for VSV therapy of B16 melanoma. *Gene Ther.* 17, 158–170.
15. Janelle, V., Langlois, M.P., Lapierre, P., Charpentier, T., Poliquin, L., and Lamarre, A. (2014). The strength of the T cell response against a surrogate tumor antigen induced by oncolytic VSV therapy does not correlate with tumor control. *Mol. Ther.* 22, 1198–1210.
16. Shen, W., Patnaik, M.M., Ruiz, A., Russell, S.J., and Peng, K.W. (2016). Immunovirotherapy with vesicular stomatitis virus and PD-L1 blockade enhances therapeutic outcome in murine acute myeloid leukemia. *Blood* 127, 1449–1458.
17. Wollmann, G., Ozduman, K., and van den Pol, A.N. (2012). Oncolytic virus therapy for glioblastoma multiforme: concepts and candidates. *Cancer J.* 18, 69–81.
18. Stojdl, D.F., Lichty, B., Knowles, S., Marius, R., Atkins, H., Sonenberg, N., and Bell, J.C. (2000). Exploiting tumor-specific defects in the interferon pathway with a previously unknown oncolytic virus. *Nat. Med.* 6, 821–825.
19. Balachandran, S., and Barber, G.N. (2000). Vesicular stomatitis virus (VSV) therapy of tumors. *IUBMB Life* 50, 135–138.
20. Johnson, J.E., Nasar, F., Coleman, J.W., Price, R.E., Javadian, A., Draper, K., Lee, M., Reilly, P.A., Clarke, D.K., Hendry, R.M., and Udem, S.A. (2007). Neurovirulence properties of recombinant vesicular stomatitis virus vectors in non-human primates. *Virology* 360, 36–49.
21. Wollmann, G., Drokhyansky, E., Davis, J.N., Cepko, C., and van den Pol, A.N. (2015). Lassa-vesicular stomatitis chimeric virus safely destroys brain tumors. *J. Virol.* 89, 6711–6724.
22. van den Pol, A.N., Dalton, K.P., and Rose, J.K. (2002). Relative neurotropism of a recombinant rhabdovirus expressing a green fluorescent envelope glycoprotein. *J. Virol.* 76, 1309–1327.
23. Muik, A., Stubbert, L.J., Jahedi, R.Z., Geiß, Y., Kimpel, J., Dold, C., Tober, R., Volk, A., Klein, S., Dietrich, U., et al. (2014). Re-engineering vesicular stomatitis virus to abrogate neurotoxicity, circumvent humoral immunity, and enhance oncolytic potency. *Cancer Res.* 74, 3567–3578.
24. Zhang, X., Zhang, T., Davis, J.N., Marzi, A., Marchese, A.M., Robek, M.D., and van den Pol, A.N. (2020). Mucin-like domain of Ebola virus glycoprotein enhances selective oncolytic actions against brain tumors. *J. Virol.* 94, e01967–e19.
25. Zhang, X., Mao, G., and van den Pol, A.N. (2018). Chikungunya-vesicular stomatitis chimeric virus targets and eliminates brain tumors. *Virology* 522, 244–259.
26. Verhaak, R.G., Hoadley, K.A., Purdom, E., Wang, V., Qi, Y., Wilkerson, M.D., Miller, C.R., Ding, L., Golub, T., Mesirov, J.P., et al.; Cancer Genome Atlas Research Network (2010). Integrated genomic analysis identifies clinically relevant subtypes of glioblastoma characterized by abnormalities in PDGFRA, IDH1, EGFR, and NF1. *Cancer Cell* 17, 98–110.
27. Wang, Q., Hu, B., Hu, X., Kim, H., Squatrito, M., Scarpace, L., deCarvalho, A.C., Lyu, S., Li, P., Li, Y., et al. (2017). Tumor Evolution of Glioma-Intrinsic Gene Expression Subtypes Associates with Immunological Changes in the Microenvironment. *Cancer Cell* 32, 42–56.e6.
28. Patel, A.P., Tirosh, I., Trombetta, J.J., Shalek, A.K., Gillespie, S.M., Wakimoto, H., Cahill, D.P., Nahed, B.V., Curry, W.T., Martuza, R.L., et al. (2014). Single-cell RNA-seq highlights intratumoral heterogeneity in primary glioblastoma. *Science* 344, 1396–1401.
29. Kim, S.S., Pirolo, K.F., and Chang, E.H. (2015). Isolation and culturing of glioma cancer stem cells. *Curr. Protoc. Cell Biol.* 67, 23.10.1–23.10.10.
30. Bao, S., Wu, Q., McLendon, R.E., Hao, Y., Shi, Q., Hjelmeland, A.B., Dewhirst, M.W., Bigner, D.D., and Rich, J.N. (2006). Glioma stem cells promote radioresistance by preferential activation of the DNA damage response. *Nature* 444, 756–760.
31. Liu, G., Yuan, X., Zeng, Z., Tunici, P., Ng, H., Abdulkadir, I.R., Lu, L., Irvin, D., Black, K.L., and Yu, J.S. (2006). Analysis of gene expression and chemoresistance of CD133+ cancer stem cells in glioblastoma. *Mol. Cancer* 5, 67.
32. Wakimoto, H., Kesari, S., Farrell, C.J., Curry, W.T., Jr., Zaupa, C., Aghi, M., Kuroda, T., Stemmer-Rachamimov, A., Shah, K., Liu, T.-C., et al. (2009). Human glioblastoma-derived cancer stem cells: establishment of invasive glioma models and treatment with oncolytic herpes simplex virus vectors. *Cancer Res.* 69, 3472–3481.
33. Carey, B.L., Ahmed, M., Puckett, S., and Lyles, D.S. (2008). Early steps of the virus replication cycle are inhibited in prostate cancer cells resistant to oncolytic vesicular stomatitis virus. *J. Virol.* 82, 12104–12115.
34. Moerdyk-Schauwecker, M., Shah, N.R., Murphy, A.M., Hastie, E., Mukherjee, P., and Grdzelskivili, V.Z. (2013). Resistance of pancreatic cancer cells to oncolytic vesicular stomatitis virus: role of type I interferon signaling. *Virology* 436, 221–234.
35. Ferluga, S., Tomé, C.M., Herpai, D.M., D’Agostino, R., and Debinski, W. (2016). Simultaneous targeting of Eph receptors in glioblastoma. *Oncotarget* 7, 59860–59876.
36. Debinski, W., and Gibo, D.M. (2005). Fos-related antigen 1 modulates malignant features of glioma cells. *Mol. Cancer Res.* 3, 237–249.
37. Jae, L.T., Raaben, M., Riemersma, M., van Beusekom, E., Blomen, V.A., Velds, A., Kerkhoven, R.M., Carette, J.E., Topaloglu, H., Meinecke, P., et al. (2013). Deciphering the glycosylome of dystroglycanopathies using haploid screens for lassa virus entry. *Science* 340, 479–483.
38. Kopecky, S.A., Willingham, M.C., and Lyles, D.S. (2001). Matrix protein and another viral component contribute to induction of apoptosis in cells infected with vesicular stomatitis virus. *J. Virol.* 75, 12169–12181.
39. Lyles, D.S. (2015). Cytopathogenesis of rhabdoviruses. In *Biology and Pathogenesis of Rhabdoviruses*, A.K. Pataik and M.A. Whitt, eds. (Hackensack, NJ: World Scientific), pp. 141–169.
40. Bayne, R.S., Puckett, S., Rodrigues, L.U., Cramer, S.D., Lee, J., Furdulj, C.M., Chou, J.W., Miller, L.D., Ornelles, D.A., and Lyles, D.S. (2020). MAP3K7 and CHD1 Are Novel Mediators of Resistance to Oncolytic Vesicular Stomatitis Virus in Prostate Cancer Cells. *Mol. Ther. Oncolytics* 17, 496–507.
41. Stojdl, D.F., Lichty, B.D., tenOever, B.R., Paterson, J.M., Power, A.T., Knowles, S., Marius, R., Reynard, J., Poliquin, L., Atkins, H., et al. (2003). VSV strains with defects in their ability to shutdown innate immunity are potent systemic anti-cancer agents. *Cancer Cell* 4, 263–275.
42. Yu, N., Puckett, S., Antinozzi, P.A., Cramer, S.D., and Lyles, D.S. (2015). Changes in Susceptibility to Oncolytic Vesicular Stomatitis Virus during Progression of Prostate Cancer. *J. Virol.* 89, 5250–5263.
43. Nguyễn, T.L.-A., Abdelbary, H., Arguello, M., Breitbach, C., Leveille, S., Diallo, J.-S., Yasmee, A., Bismar, T.A., Kirn, D., Falls, T., et al. (2008). Chemical targeting of the innate antiviral response by histone deacetylase inhibitors renders refractory cancers sensitive to viral oncolysis. *Proc. Natl. Acad. Sci. USA* 105, 14981–14986.
44. Shulak, L., Beljanski, V., Chiang, C., Dutta, S.M., Van Grevenynghe, J., Belgnaoui, S.M., Nguyễn, T.L.-A., Di Lenardo, T., Semmes, O.J., Lin, R., and Hiscott, J. (2014).

- Histone deacetylase inhibitors potentiate vesicular stomatitis virus oncolysis in prostate cancer cells by modulating NF- κ B-dependent autophagy. *J. Virol.* *88*, 2927–2940.
45. Muscolini, M., Castiello, L., Palermo, E., Zevini, A., Ferrari, M., Olgner, D., and Hiscott, J. (2019). SIRT1 Modulates the Sensitivity of Prostate Cancer Cells to Vesicular Stomatitis Virus Oncolysis. *J. Virol.* *93*, e00626-e19.
 46. Mootha, V.K., Lindgren, C.M., Eriksson, K.F., Subramanian, A., Sihag, S., Lehar, J., Puigserver, P., Carlsson, E., Ridderstråle, M., Laurila, E., et al. (2003). PGC-1 α -responsive genes involved in oxidative phosphorylation are coordinately downregulated in human diabetes. *Nat. Genet.* *34*, 267–273.
 47. Subramanian, A., Tamayo, P., Mootha, V.K., Mukherjee, S., Ebert, B.L., Gillette, M.A., Paulovich, A., Pomeroy, S.L., Golub, T.R., Lander, E.S., and Mesirov, J.P. (2005). Gene set enrichment analysis: a knowledge-based approach for interpreting genome-wide expression profiles. *Proc. Natl. Acad. Sci. USA* *102*, 15545–15550.
 48. Yale University School of Medicine (2020). In Memoriam: Anthony N. van den Pol, PhD 1949–2020, https://medicine.yale.edu/profile/anthony_vandenpol/.